Jurnal Teknologi

Full Paper

OPTIMIZATION OF CELLULOSE NANOCRYSTALS (CNC)/POLYCAPROLACTONE (PCL) NANOFIBER SCAFFOLDS FOR ENHANCED TISSUE ENGINEERING APPLICATIONS

Mohamed Hasaan Hussain[a], Noor Fitrah Abu Bakar[a]*, Norazah Abd Rahman[a], Muhammad Huzaimi Haron[b], Huey Ling Tan[a], Lay Kek Teh[c,d]

[a]School of Chemical Engineering, College of Engineering, Universiti Teknologi MARA, 40450, Shah Alam, Selangor, Malaysia
[b]Department of Pharmacology, Faculty Medicine, Universiti Teknologi MARA Cawangan Selangor, Sungai Buloh Campus, 47000 Selangor, Sungai Buloh, Malaysia
[c]Integrative Pharmacogenomics Institute, Universiti Teknologi MARA Cawangan Selangor, Puncak Alam Campus, 42300 Puncak Alam, Selangor, Malaysia
[d]Faculty of Pharmacy, Universiti Teknologi MARA Cawangan Selangor, Puncak Alam Campus, 42300 Puncak Alam, Selangor, Malaysia

Article history
Received
9 July 2024
Received in revised form
26 February 2025
Accepted
7 March 2025
Published Online
24 October 2025

*Corresponding author
fitrah@uitm.edu.my

Graphical abstract

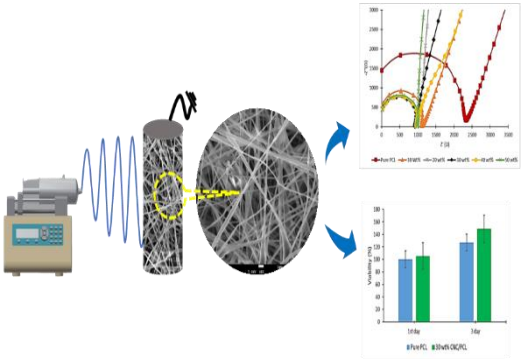

Abstract

Cellulose, an abundantly available and biocompatible material, holds great promise for tissue engineering scaffolds due to its excellent physicochemical properties, low toxicity, and good biocompatibility. This study systematically explores the optimization of cellulose nanocrystals (CNC) and polycaprolactone (PCL) electrospun nanofiber scaffolds for tissue engineering applications. Key physical properties such as fiber diameter, porosity, wettability, thermal degradability, and ionic conductivity were comprehensively assessed, focusing on tuning the concentration of CNC from 0 to 50 wt%, a pivotal parameter in the electrospinning process. Results reveal that adding CNC to CNC/PCL nanofiber scaffolds reduced fibre diameter and increased wettability and porosity. Field emission scanning electron microscopy (FESEM) characterizations demonstrate a reduction in fiber diameters with escalating CNC concentration, producing nanofibers with diameters below 200 nm when 50 wt% of CNC is incorporated. Electrochemical impedance spectroscopy (EIS) findings highlight an enhanced ionic conductivity in CNC/PCL scaffolds, showing a twofold increase compared to pure PCL nanofibers. Differential scanning calorimetry (DSC) analysis indicates that the melting temperature of all samples exceeds body temperature, ideal for tissue engineering applications. Biocompatibility evaluation using RAW 264.7 cells demonstrates that the 30wt% CNC/PCL scaffold enhances cell survival rate and proliferation compared to PCL nanofibers. These findings suggest that the fabricated CNC/PCL nanofiber scaffolds have the potential to be applied in diverse tissue engineering scenarios, contributing to advancements in regenerative medicine.

Keywords: Cellulose nanocrystal, Electrospinning, Nanofiber, Scaffold

Abstrak

Selulosa merupakan bahan yang sangat banyak didapati dan bahan bioserasi yang mempunyai potensi untuk pembuatan struktur kejuruteraan tisu kerana sifat fizikokimia yang baik, ketoksikan yang rendah, dan kekuatan mekanikal yang tinggi. Kajian ini secara sistematik meneroka pengoptimuman nanoserat selulosa (CNC) dan struktur nanoserat elektroputar *polycaprolactone* (PCL) untuk aplikasi kejuruteraan tisu. Sifat fizikal utama seperti diameter serat, keliangan, kebolehbasahan, kebolehuraian termal, dan kekonduksian ionik dinilai secara menyeluruh, dengan penumpuan kepada penalaan kepekatan CNC daripada 0 hingga 50 wt% yang merupakan parameter penting dalam proses elektroputaran. Keputusan menunjukkan bahawa penggunaan CNC dalam struktur nanoserat CNC/PCL menyebabkan peningkatan diameter serat, kebolehbasahan, dan keliangan. Pencirian mikroskop elektron pengimbasan pancaran medan (FESEM) menunjukkan pengurangan diameter serat dengan peningkatan kepekatan CNC dan menghasilkan nanoserat dengan diameter di bawah 200 nm apabila 50 wt% CNC digunakan. Penemuan spektroskopi impedans elektrokimia (EIS) menunjukkan peningkatan kekonduksian ionik dalam struktur CNC/PCL, menunjukkan peningkatan dua kali ganda berbanding nanoserat PCL tulen. Analisis kalorimetri pengimbasan pembezaan (DSC) menunjukkan bahawa suhu lebur semua sampel melebihi suhu badan yang sesuai untuk aplikasi kejuruteraan tisu. Penilaian kebioserasian menggunakan sel RAW 264.7 menunjukkan bahawa struktur 30wt% CNC/PCL meningkatkan pengembangbiakan sel berbanding nanoserat PCL tulen. Penemuan ini menunjukkan bahawa struktur nanoserat CNC/PCL yang dihasilkan berpotensi untuk digunakan dalam pelbagai senario kejuruteraan tisu yang dapat menyumbang kepada kemajuan dalam bidang perubatan janasemula.

Kata kunci: Selulosa nanokristal, pemutaran elektrik, nanofiber, perancah

1.0 INTRODUCTION

Scaffold technology is crucial in modern tissue engineering solutions and regenerative medicine. Biomaterials that closely mimic the extracellular matrix (ECM) enhance cell proliferation, migration, and growth, promoting efficient tissue regeneration. These materials improve cellular interactions and outcomes in regenerative medicine by replicating ECM properties.[1]. Research shows that among the array of biomaterials explored for scaffold fabrication, natural polymer-based materials emerged as promising candidates due to their high biocompatibility, renewability, and less toxicity [2,3]. In this context, nanocellulose and its derivatives show excellent biocompatibility and lower toxicity. Notably, cellulose material-based electrospun nanofiber scaffolds are addressed as a versatile platform due to their high surface area, optimizable physical properties, and resemblance to the morphologies of natural ECM [4,5].

Nanocrystalline cellulose (CNC) and fibrillated nanocellulose, derived from cellulose pulps, with bacterial cellulose (BC) extracted from microorganisms, are categorized as nanocellulose. [6]. Abundant and readily available hydroxide (– OH) functional groups on the nanocellulose surfaces can be easily modified with various chemically active functional groups that mimic the biochemical structure of native ECM, proteoglycans, and other cellular components [7,8]. Furthermore, fibrillated morphology, easily combined with other polymers to produce nanocomposites, high water retention properties, hydrophilicity, and high mechanical strength make them the ultimate material for tissue engineering scaffold and drug delivery applications[8–10]. Furthermore, nanocellulose combined with conductive nanoparticles such as graphene and gold composites exhibits high electrical conductivity while maintaining lower toxicity compared to conventional conductive polymers such as polyaniline (PANI) and poly(3,4-ethylene dioxythiophene) (PEDOT) for conductive tissue engineering scaffold applications, implantable biosensors, and neural interfaces [11–13]. Nanocrystalline cellulose or nanowhiskers are cellulose-based nanocrystals isolated from highly crystalline regions of cellulose through processes such as acid hydrolysis or high-energy milling [14,15]. This type of nanocrystalline cellulose can bind with drug molecules and antibodies through their abundant reactive ends, including modified SO^{2-}, NH_2 and functional polymer groups, and its high surface area acts as an excellent drug delivery vehicle [16].

Furthermore, CNC is modified with fluorescent molecules and utilized for bioimaging analysis [17]. In addition, CNC is added as fillers to various polymer mixtures to enhance mechanical strengths and physical properties, which are suitable for developing scaffolds for hard tissue such as cartilage and, bone tissue regeneration and prosthetic surfaces [18,19]. In this context, adding CNC with biopolymers such as polycaprolactone (PCL)confers great potential for developing tissue engineering scaffolds with optimum physical properties, biocompatibility, and less toxicity.

Besides, Topographical features and morphology of tissue engineering scaffolds play a vital role in mimicking the natural tissue environment and ECM. Electrospinning nanofibers can efficiently recreate the morphology of ECM. Electrospinning is an efficient technology for producing nanofiber with optimum physical properties from a viscous polymer precursor solution by applying high electric voltage [20]. Numerous studies have proved that electrospun nanofiber with nanometric scale fiber diameter and two-dimensional and continuous nanostructure mimics the topographical features of key tissue components, such as collagen fibril structure and the hierarchical architecture of ECM [21]. Additionally, the porosity, surface area and diameter of electrospun nanofibers can be easily optimized by varying electrospinning parameters such as applied voltage, polymer concentration, conductivity of the precursor solution, and electrospinning working distance. The higher surface area and high porosity of electrospun nanofibers allow the coating of various biologically active molecules, such as proteins, antibodies, drugs, and ligands, onto electrospun scaffolds. Electrospinning technology allows the synthesis of nanofibers from polymer solutions doped with nanoparticles, which confers an excellent opportunity to synthesize nanocomposite scaffolds with exceptional properties. Notably, CNC-doped PCL nanofiber scaffolds stand out for their improved mechanical strength and high biocompatibility and biodegradability of both CNC and PCL [22,23].

Electrospinning of CNC/PCL composites has already been studied, primarily focusing on CNC as a reinforcing additive (0.5–20 wt%) to enhance the mechanical properties of PCL, resulting in nanofiber diameters typically exceeding 500 nm [22–26]. Despite the promising outcomes of these studies, further improvements are necessary to optimize scaffold properties such as fiber diameter, porosity, and ionic conductivity, which are crucial for scaffold functionality in tissue regeneration. However, this study explores CNC as a primary component in CNC/PCL nanofiber scaffolds, with CNC concentrations ranging from 0 to 50 wt%. Unlike previous studies, we emphasize CNC's role beyond a mere additive, examining its effects on reducing fiber diameter (achieving an approximate 200 nm diameter at higher concentrations) and increasing the scaffold's ionic conductivity, a feature essential for bioelectrical interactions in electroactive tissue applications. In addition, our study comprehensively analyses key properties—porosity, wettability, and thermal stability—tailored for tissue engineering applications. By advancing the understanding of CNC as a central component rather than an additive, our findings present a distinctive approach to optimizing CNC/PCL nanofiber scaffolds, broadening their potential for more effective and functional scaffold designs in regenerative medicine.

Overall, this study investigates the physical and biocompatibility of cellulose nanocrystal/PCL composite electrospun nanofiber scaffolds for tissue engineering applications. The primary objective is to manipulate critical parameters, such as electrospinning conditions and CNC concentration, that could influence the physical properties and biocompatibility of the resulting scaffolds, aligning with the specifications of regenerative medicine. The fabricated CNC-based nanofiber scaffold, with carefully tuned porosity, morphology, thermal degradability and biocompatible surface facilitating cell adhesion, holds significant potential for enhancing tissue regeneration.

2.0 METHODOLOGY

2.1 Materials

Polycaprolactone (average Mn 80,000)) was purchased from Sigma – Aldrich, Germany. Cellulose Nanocrystal (Nanocrystalline Cellulose, CNC) wide: 10-20 nm, length: 300-900 nm, Dry powder was purchased from Nanografi Nano Teknoloji AS, Germany. Solvents acetone ≥99.5% and Dimethylformamide (DMF) (≥99.9%) were purchased from Merk, Germany. Dulbecco's Modified Eagle Medium (DMEM) supplemented with 5% (v/v) fetal bovine serum (FBS) and phosphate-buffered saline was purchased from Lonza, US. Antibiotics and penicillin/streptomycin solution were purchased from Science, USA. RAW 264.7 cell line was obtained from Integrative Pharmacogenomics Institute, Universiti Teknologi MARA, Puncak Alam Campus, Malaysia.

2.2 Synthesis of CNC/PCL Electrospun Nanofiber

CNC/PCL nanofiber scaffold matrix was fabricated using the electrospinning technique. Figure 1 depicts an electrospinning instrument setup using a high-voltage power supply, syringe pump, counter electrode, and metal nozzle. 12 wt% of PCL and CNC were dissolved in a 7:3 acetone-DMF mixture under stirring at 600 rpm overnight, a duration determined through trial and error. The two components were combined at mass ratios of CNC to PCL (1:9, 2:8, 3:7, 4:6, and 5:5), maintaining a total polymer concentration of 12 wt%, to synthesize electrospun nanofiber scaffolds with CNC to PCL weight percentages of 0%, 10%, 20%, 30%, 40%, and 50%. A 5ml syringe with a 22-gauge blunt-tipped needle was filled with different concentrations of CNC-dispersed CNC/PCL precursor solutions separately. The precursor

solution in the syringe was installed on the syringe pump. The voltage applied to the spinneret (metal nozzle) was set to 17 kV for synthesizing neat PCL nanofibers and 15 kV for CNC/PCL nanofibers with CNC concentrations ranging from 10 to 50 wt%. The syringe pump flow rate was set to 0.8 ml/h for neat PCL and 1 ml/h for CNC/PCL nanofibers with 10 to 50 wt% CNC. The distance between the spinneret and the grounded collector was maintained at 15 cm. Finally, electrospun nanofibers were deposited on the aluminium foil-covered rotating drum collector at 200 rpm rotating speed.

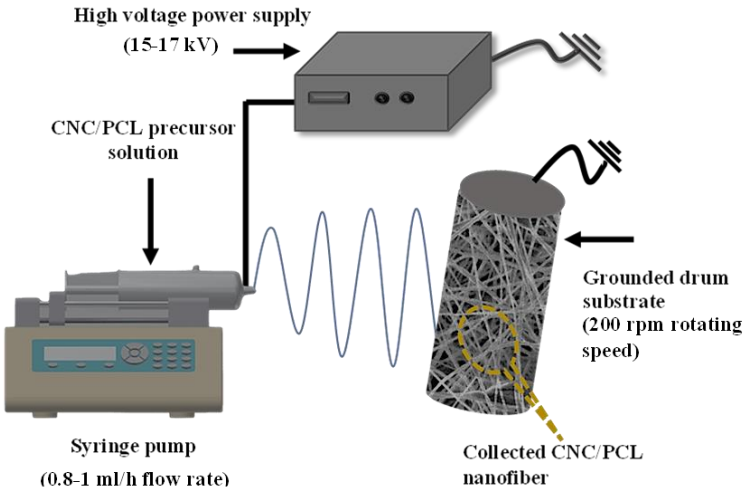

Figure 1 Schematic diagram of CNC/PCL electrospinning nanofiber scaffold synthesis process

2.3 Characterizations Performed

2.3.1 Field Emission Scanning Electron Microscopy (FESEM)

The morphology of varying weight percentages of CNC/PCL composite electrospun fiber was examined employing a field emission scanning electron microscope (FESEM, Pressure Zeiss Supra 35 model). Before FESEM analysis, the samples were coated with a 15 nm-thick layer of gold using sputter-coating. During the image processing, the FESEM was operating at an accelerating voltage of 5 kV to capture the images. A magnification of 10,000x was used to observe the overall morphology, fiber uniformity, and general structure of the scaffold.

ImageJ software (version 1.8.0_172) was utilized for FESEM image morphology analysis and fiber diameter measurement. During the ImageJ image analysis, 100 fibers from the FESEM images of each sample were selected to obtain mean and standard deviation values.

2.3.2 Water Contact Angle Measurement

The wettability properties of the Different weight percentages of CNC/PCL nanofiber composition electrospun nanofiber scaffold were assessed by a water contact angle analysis by following the methodology given in the reference [27]. During the analysis, the samples were positioned on the sample stage of the goniometer (goniometer AST/VCA-3000S), and a charge-coupled device (CCD) camera was utilized to photograph the profile of water droplets on the scaffold. During the WCA analysis, 5 µl of double DI water droplet was placed on the samples and Three contact angle measurements were taken at various locations on the sample at 60 s time interval after droplet was dispensed. The average of these measurements was accounted as a final value of the water contact angle.

2.3.3 Porosity Analysis

The liquid uptake method, previously documented in the literature [20,23], was employed to ascertain the bulk porosity of CNC/PCL nanofiber composition scaffolds with varying concentrations. Porosity evaluation involved cutting electrospun fiber mats into 2 cm × 2 cm squares, submerging them in n-butanol at room temperature for 2 hours, removing them from the solution, drying them with tissue, and subsequently weighing them. Equation (1) was then used to calculate the porosity of these fiber mats.

$$Porosity(\%) = \frac{m_b/\rho_b}{(m_b/\rho_b)+(m_s/\rho_s)} \times 100\% \quad (1)$$

Where m_p and m_b are the masses of CNC/PCL scaffolds before and after soaking in n-butanol solvent, respectively. Similarly, ρ_b represents the density of n-butanol, and ρ_s refers to the density of the scaffold skeleton, respectively.

2.3.4 Swelling Ratio Analysis

The in vitro swelling analysis of scaffolds was conducted following the methodology described in the previous literature [28][29]Briefly, Different weight percentages of CNC/PCL nanofiber composition electrospun nanofibrous mats with dimensions 2 cm × 2 cm were immersed in a phosphate buffer saline (PBS) solution for 24 hours. This immersion process took place within a shaking incubator set at 37 °C.

The percentage of the swelling ratio (SR) of scaffolds was determined using the equation (2):

$$SR = \frac{W_s - W_b}{W_b} \times 100 \quad (2)$$

Where W_s represents the weight of the nanofibrous after swelling, and W_b denotes the initial weight of the dry mat.

2.3.5 FTIR Analysis

The chemical structure of PCL nanofibers with varying CNC weight percentages was analyzed using Fourier-transform infrared (FTIR) spectroscopy (Perkin Elmer Spectrum One). FTIR spectra were collected by

recording absorption signals in the 4000–500 cm^{-1} range at 4 cm^{-1} resolution.

2.3.6 DSC Analysis

The thermal degradation characteristics of CNC/PCL nanofiber scaffolds with different weight percentages were investigated using a differential scanning calorimeter (DSC, the Q1000 apparatus from TA Instruments, USA). During the degradation analysis, DSC was operated under an N2 gas flow rate of 50 mL/min and a scanning rate of 10 °C/min. Melting point determination was carried out using 10 mg of CNC/PCL samples.

2.3.7 Electrochemical Impedance Spectroscopy (EIS) Analysis

The conductivity of the electrospun nanofiber scaffolds was analysed by electrochemical impedance spectroscopy (EIS) using a potentiostat instrument (Autolab pgstat204 instrument). For electrochemical EIS analysis, different weight percentages of CNC-added PCL precursor solutions were electrospun onto a screen-printed carbon electrode (SPCE) that is affixed to the collecting plate substrate of the setup. Throughout the deposition process, only the working electrode surface of the SPCE was exposed to the electrospun nanofibers, while the remaining areas were covered using aluminium foil.

The EIS characterization was carried out in a phosphate buffer solution with a concentration of 0.01 M as an electrolyte solution, with the frequency range adjusted between 100 MHz and 100 kHz. From the EIS frequency response analysis (FRA), the charge transfer resistance (Rct) of the scaffold was measured to determine the ionic conductivity (σ) of the nanofiber scaffold using equation (3) [20,30]:

$$\sigma = \frac{L}{R_{ct} \cdot A} \quad (3)$$

In equation (3), the variable L denotes the thickness of the fiber mat, which was set at 0.001 cm for this study. Rct stands for the charge transfer resistance (Ω), while A represents the contact area of the working electrode, which was determined to be 0.1257 cm2 for this experiment.

2.3.8 Cell Culture and MTT Assay

Synthesized scaffolds with varying weight percentages (0%, 10%, 20%, 30%, 40%, and 50%) of CNC-added PCL underwent sterilization via UV irradiation for 2 hours following previous studies [31,32]. These sterilized scaffolds were then cut into pieces with 1.9 cm^2 area and gently placed into sterilized 24-well plates. Each well was filled with 2 ml of cell culture medium comprising Dulbecco's Modified Eagle Medium (DMEM) supplemented with 5% (v/v) fetal bovine serum (FBS) and antibiotics (100µg/ml penicillin and 100µg/ml streptomycin). RAW 264.7 macrophages were seeded into the wells at a density of 1 × 10^5 cells per well. The cell cultures were maintained at 37°C in a humidified atmosphere with 5% CO2 for either 1 or 3 days.

To evaluate the viability of RAW 264.7 cells on different surface-modified scaffolds, an MTT (3-(4,5-dimethylthiazole-2-yl)-2,5-diphenyltetrazolium) assay was performed. Generally, the RAW 264.7 cell line, a murine macrophage model, is used for biocompatibility testing of scaffolds as it helps evaluate multiple parameters, including immune response, toxicity, cell adhesion, and inflammatory behavior [33,34]. A working solution of MTT at a concentration of 0.005 mg/ml was prepared by dissolving MTT (Sigma) in phosphate-buffered saline (PBS) and then sterilized. After the specified culture period, 100 µl of the MTT solution was added to each well containing fresh culture medium. The plates were incubated for an additional 4 hours to allow formazan crystals to form via mitochondrial dehydrogenases in viable cells. Subsequently, the culture medium was aspirated, and 100 µl of dimethyl sulfoxide (DMSO) was added to each well to dissolve the formazan crystals. The resulting solution's optical density was measured using an Elisa plate reader at a wavelength of 570 nm.

3.0 RESULTS AND DISCUSSION

3.1 Morphology and Fiber Diameter Analysis

To prepare the CNC/PCL nanofiber with bead-free nanofiber morphology, high wettability, high swelling rate and optimum physical properties, 10, 20, 30, 40 and 50 wt% of CNC were added to 12 wt% of the total polymer concentration of PCL precursor solution. Figure 2 shows the FESEM micrographs and diameter analysis of different weight percentages of CNC to PCL electrospun nanofiber. In different concentrations of CNC, pure PCL, and 10, 20, 30, 40 and 50 wt% of CNC with PCL resulted in 359.12±133 nm, 311.94±90 nm, 275.56±96 nm, 263.93±81 nm, 210.96±68 nm and 198.23±66 nm of mean diameter nanofibers respectively. These results indicate that the mean diameter of CNC/PCL electrospun nanofiber gradually decreased with the increasing concentration of CNC. In addition, a pure PCL solution produces significantly larger diameters and topographically highly heterogeneous nanofibers than CNC-added nanofibers. These results were attributed to the low conductivity of the PCL precursor solution. When CNC was introduced to the PCL precursor solution, the ionic conductivity of the precursor solution increased, reducing the electrospun nanofiber size [35]. Notably, in this study, concentrations of CNC exceeding 20 wt% resulted in the formation of narrow and thin nanofibers with less than 200 nm of diameter. These dimensions mimic the topographical features of ECM protein, such as

collagen fibrils. Therefore, it could be concluded that the mean diameter and morphological features of 20 – 50 wt% of CNC/PCL can be optimized for mimicking the topographical features of ECM tissue.

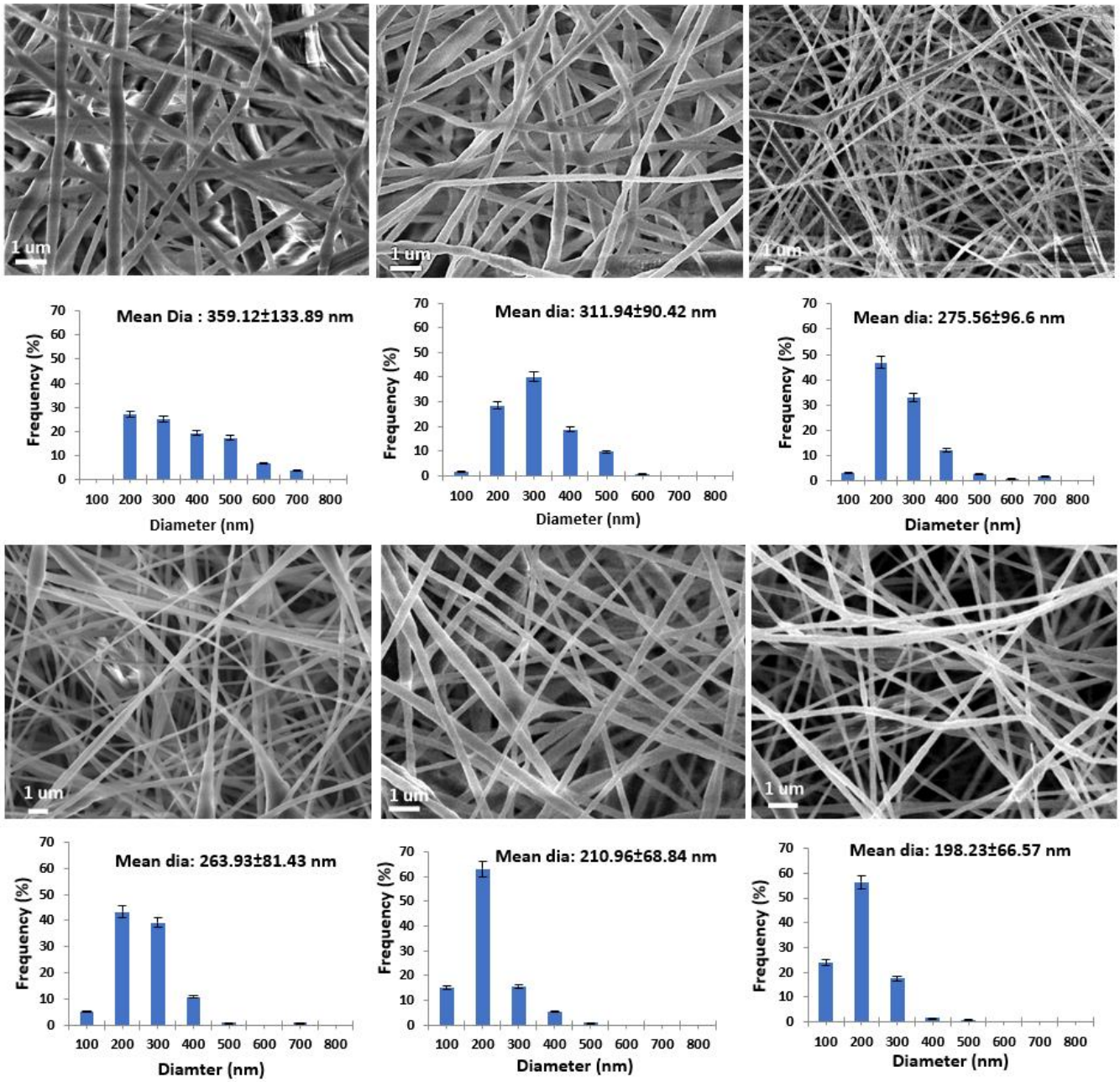

Figure 2 FESEM micrograph images CNC/PCL nanofiber with CNC content (A) 0 wt%, (B) 10 wt%, (C) 20 wt%, (D) 30 wt%, (E) 40 wt% and (F) 50 wt% of CN

3.2 Wettability Analysis

In tissue engineering applications, the wettability and hydrophilic properties of scaffolds significantly impact cell proliferation and migration processes. Hydrophilic surfaces improve cell adhesion via improving integrin-based binding, which enhances the proliferation and migration of cells [36]. In addition, hydrophilic scaffold surfaces efficiently transport nutrients, ions, oxygen, and other biological molecules [37]. Figure 3 shows the water contact angle analysis of different weight percentages of CNC to PCL electrospun nanofiber. Herein, pure PCL and CNC/PCL nanofibers with 10, 20, 30, 40 and 50 wt% of CNC exhibited contact angles of 132.15 ± 0.05˚, 125.55 ± 0.05˚, 119.6 ± 1.2˚, 98.75 ± 1.05˚, 0˚ and 0˚, respectively.

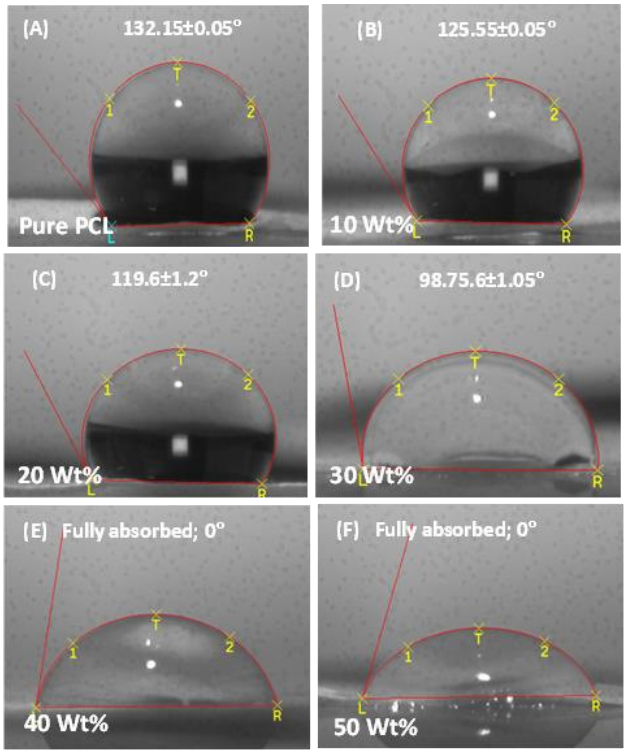

Figure 3 Water contact angle images of CNC/PCL nanofibers with (A) 0 wt%, (B) 10 wt%, (C) 20 wt%, (D) 30 wt%, and (E and F) 40 wt% and 50 wt% CNC in PCL matrices respectively, captured 2 seconds after water dispensing, as the samples absorb water. By 60 seconds, the water droplets are fully absorbed

These results indicate that pure PCL is highly hydrophobic, and the presence of CNC enhances the hydrophilicity of the nanofiber. Notably, the water contact angle decreased with increasing CNC wt%, and the nanofiber completely absorbed the water at concentrations higher than 40wt% of CNC. The primary reasons behind this higher water absorbance of 40 and 50 wt% of CNC/PCL are attributed to the higher concentration of the free – OH group in CNC. The free–OH groups form hydrogen bonds with water, leading to the absorption of a greater quantity of water molecules. However, the high water absorption capacity in the 40 and 50 wt% of CNC/PCL scaffold may pose challenges such as rapid hydrolytic degradation and burst drug release in drug delivery applications [38,39]. In addition, although high hydrophilicity can improve cell survival rates, cell-binding ECM proteins are particularly responsive to moderately hydrophobic surfaces [40,41]. Excessive hydrophilicity can reduce cell adhesion strength and limit migration, as overly hydrophilic surfaces may hinder stable ECM protein binding [40,41]. Therefore, a balanced, moderately hydrophilic surface is essential to maximize cell binding, support cell migration, and ensure effective integration with the scaffold. In this context, the results imply that a composition of 30 wt% of CNC/PCL would be optimal for producing tissue engineering scaffolds.

3.3 Porosity and Swelling Analysis

In tissue regeneration, a highly porous scaffold with a porosity greater than 90% results in faster and more effective tissue reformations [42]. Highly porous materials allow effective diffusion of biological molecules, nutrients, oxygen, and drugs, promoting cell proliferation, migration, and integration. Similarly, the highly porous surface of scaffolds improves cell adhesion to the scaffold and allows cells to migrate in a three-dimensional pathway [43]. Besides, the high swelling and water retention properties of the scaffold improve cell viability and enhance cell growth by facilitating molecular transportation in a liquid environment [44]. Table 1 shows the porosity and swelling rate of different weight percentages of the CNC to PCL nanofiber scaffolds. According to Table 1, the porosity percentages for pure PCL and CNC/PCL nanofibers with 10, 20, 30, 40 and 50 wt % were determined to be 70%, 73.72%, 79.73, 84.77, 86.53 and 93.34%, respectively. These results imply that the higher concentration of CNC in CNC/PCL nanofiber increases the porosity, and the highest wt% CNC resulted in the highest porosity, approximately 20% higher than pure PCL nanofiber. Generally, a smaller diameter of nanofiber exhibited higher interiority and high electrical conductivity of precursor solution, evaporating more solvent from nanofiber and resulting in high inter-porosity. Therefore, it is apparent that the higher weight percentage of CNC resulted in a minimum nanofiber diameter with high inter and intra porosity. In addition, we hypothesize that the CNC/PCL nanofiber may contribute to a reduction in crystallinity, potentially increasing the inter-porosity of the nanofiber. These results align with the observed swelling rate of various wt% of CNC/PCL electrospun nanofiber scaffolds. According to Table 1, the swelling percentages for pure PCL and 10, 20, 30, 40 and 50 wt % of CNC/PCL nanofibers were 16.67%, 323.26%, 359.18%, 362.26%, 376.36 and 392.31, respectively. The highest swelling percentage was obtained in the nanofiber with the highest CNC content. The higher porosity and enhanced water absorption capability of cellulose confer remarkable water swelling properties of the CNC/PCL electrospun nanofiber.

Table 1 Porosity and water swelling percentage of different weight percentages of CNC to PCL electrospun nanofiber

Sample	Porosity (%)	Swelling (%)
Pure PCL	70.09±8.16	16.67±3.81
10wt% CNC	73.72±12.32	323.26±29.2
20wt% CNC	79.73±13.58	359.18±22.17
30wt% CNC	84.77±13.01	362.26±31.4
40wt% CNC	86.53±18.73	376.36±39.65
50wt% CNC	93.34±15.61	392.31±38.58

3.4 FTIR Analysis

The fiber mats were analyzed using FTIR spectroscopy to validate the molecular interaction of PCL and CNC in CNC/PCL fibers. As shown in Figure 4, the characteristic peaks corresponding to the functional group of both PCL and CNCs were observed, with noticeable shifts in these peaks. These observations suggest the interaction between PCL and CNC and the formation of CNC/PCL nanocomposites. According to Figure 4, characteristic absorbance peaks at 3342 and 1162 cm^{-1} wavenumbers represent the hydrogen-bond O-H stretching and C-O-C asymmetric valence vibration of the CNC and PCL molecules, respectively. Notably, the carbonyl stretching absorption of pure PCL electrospun nanofiber appeared at about 1720 cm^{-1}, but it shifted to a higher wavenumber around 1725 cm^{-1} in 50 wt% CNC added PCL nanocomposite fiber mats (As shown in Figure 5). Generally, FTIR carbonyl stretching of PCL molecules at 1720 cm^{-1} arises from the composition of crystalline and amorphous phases of the PCL molecules [22]. Herein, the amorphous phase carbonyl group of PCL appeared at a higher wavelength than the crystalline phase stretching. Therefore, the stretching shift of the carbonyl group from 1720 cm^{-1} to 1725 cm^{-1} implies an increase in the amorphous phase of PCL within the CNC/PCL composite fiber mats.

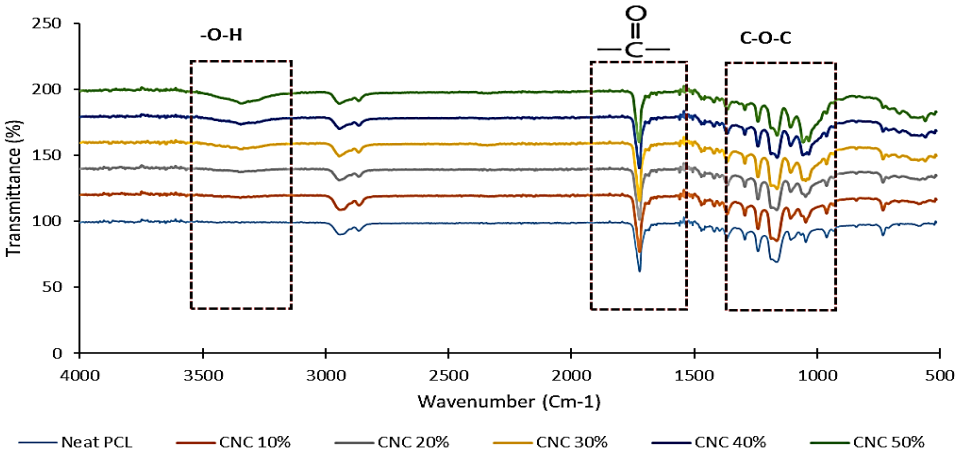

Figure 4 FTIR analysis of 0, 10, 20, 30, 40 and 50 wt% of CNC-added PCL nanofiber

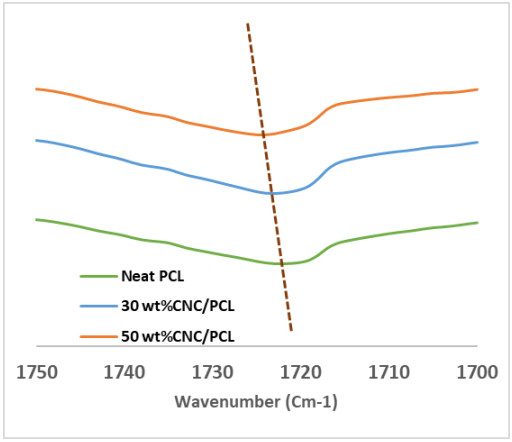

Figure 5 Shift of the carbonyl group in the FTIR spectra of neat PCL and CNC-added PCL nanofibers at different weight percentages

3.5 Thermal Degradability Analysis

Figure 6 shows the DSC thermograms of different weight percentages of CNC-loaded PCL electrospun nanofibers. All compositions, ranging from 10 to 50 wt% of CNC with PCL and pure PCL electrospun nanofibers, exhibit almost similar melting temperatures (T_m) around 61.5 °C, which is higher than the human body's physiological temperature. Nevertheless, the addition of CNC in PCL nanofibers resulted in a slight decrease in melting temperature compared to pure PCL nanofibers. This reduction is attributed to the lower melt viscosity of CNC particles, resulting from a decrease in the degree of crystallinity of the PCL by controlling or prohibiting the moment of polymer segments. These findings are consistent with the results

obtained from FTIR analysis [45]. However, the DSC results imply that the good miscibility of CNC and PCL polymers and the melting temperature of CNC/PCL composite are optimal for tissue engineering scaffold applications [45].

3.6 Ionic Conductivity Analysis of Different Weight Percentages of CNC/PCL Nanofiber Matrices

Ionic conductivity plays a crucial role in tissue engineering, particularly in designing scaffolds for applications involving electroactive tissues or cells. Ionic conductivity refers to the ability of a material to conduct ions, such as sodium (Na^+), potassium (K^+), calcium (Ca^{2+}), chloride (Cl^-), and other ions that play critical roles in various physiological processes [46]. In tissue engineering, the ionic conductivity of a scaffold can be essential for several reasons, such as electrical stimulation, cell communication, electroactive tissues, and drug delivery [46,47]. Generally, PCL is electrically inert, and its highly hydrophobic properties are less favourable for ionic conductivity. However, when CNC is dopped with PCL in electrospun nanofibers, the ionic conductivity of the resulting compositions (0, 10, 20, 30, 40 and 50 wt%CNC-added PCL nanofiber) was determined using their charge transfer resistance obtained from Nyquist plot, as shown in Figure 7, i.e. 2331.14 Ω, 1109.18 Ω, 941.26 Ω, 917.46 Ω, 977.65 Ω and 987.178 Ω, respectively. The conductivity of pure PCL nanofiber and the nanofiber matrices with 0, 10, 20, 30, 40 and 50 wt% CNC additions were found to be 3.41×10^{-5} S/cm, 7.17×10^{-5} S/cm, 8.45×10^{-5} S/cm, 8.67×10^{-5} S/cm, 8.13×10^{-5} S/cm and 8.05×10^{-6} S/cm, respectively as shown in Figure. 8. The conductivity of PCL nanofiber nearly twofold increased from 3.41×10^{-5} S/cm to 7.17×10^{-5} S/cm with the addition of 10 wt% of CNC. The conductivity of nanofiber continued to increase with higher weight percentages of CNC in the composite. While pure CNC is inherently less conductive, the hydrophilic nature of cellulose and CNCs promotes the interaction of water molecules with ions. This interaction, known as ion hydration, aids in solvating and transporting ions through the membrane, thereby enhancing conductivity. Furthermore, the high surface area of CNCs, attributed to their nanoscale dimensions and unique rod-like structure, offers increased opportunities for ions to interact with the membrane, further promoting ion transport. In addition, incorporating CNCs into electrospun nanofiber creates a network of nanoscale channels or pores within the membrane, facilitating the movement of ions and enabling smoother ion transport through the membrane [48,49]. Notably, 30 wt% CNC shows the highest ionic conductivity, and the addition of CNC beyond this concentration results in a slight decrease in the ionic conductivity of CNC/PCL nanofiber composite. This observed increment in conductivity is presumed to be linked to the aggregation of CNC particles in higher concentrations. However, adding CNC particles to PCL nanofibers resulted in a two-fold increase in ionic conductivity compared to neat PCL electrospun nanofibers. This enhanced conductivity meets the minimum requirements for improving conductive tissue regeneration, such as nerve tissue recovery, thereby highlighting the potential of [50, 51].

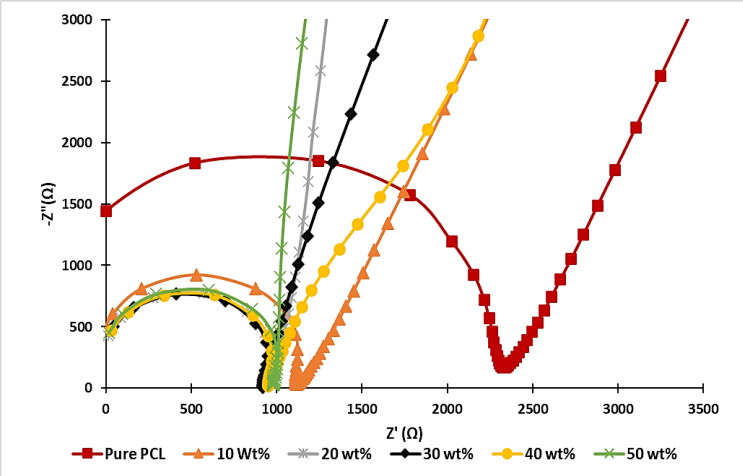

Figure 7 EIS Nyquist plots of 10 – 50 wt% of CNC added PCL electrospun nanofiber composite scaffold

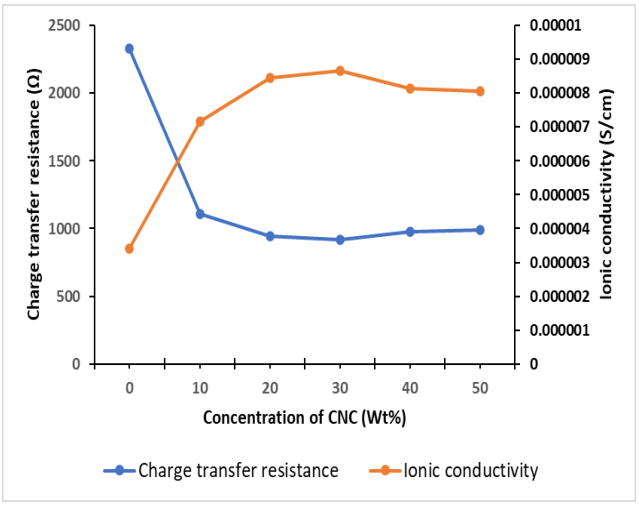

Figure 8 The charge transfer resistance and ionic conductivity of the different percentages of CNC-added PCL electrospun nanofibers

3.7 Cell Viability on Different Weight Percentages of CNC/PCL Scaffolds

The MTT cell viability assay was conducted to compare the viability of RAW 264.7 cells on 30 wt% CNC/PCL and pure PCL scaffolds, following existing literature [52,53]. Figure 9 shows that the chart illustrates cell viability over two-time points (1st day and 3rd day) for two material types: Neat PCL and a 30 wt% CNC/PCL composite. On the first day, both materials showed similar cell viability, with the CNC/PCL composite showing a slightly higher percentage than Neat PCL, indicating that the addition of cellulose nanocrystals (CNC) might support initial cell survival. By the third day, cell viability

has increased for both materials, but this effect is more pronounced in the CNC/PCL composite, which reaches close to 140% viability, compared to Neat PCL, which also rises but to a slightly lower level. This trend suggests that the CNC/PCL composite not only maintains but enhances cell viability over time, potentially due to the bioactivity of CNC, which may improve cell proliferation or compatibility. Overall, the addition of CNC to PCL seems beneficial for cell viability, making the composite a promising material for applications where cell growth and compatibility are essential. The results of this study align with existing literature where human bone marrow-derived mesenchymal stem cells (hMSCs) cultured on CNC/PCL composites exhibited a cell viability and proliferation pattern similar to our current study. However, it is important to note that in this work, the CNC/PCL scaffold was prepared using only 2 wt% of CNC doped with PCL [54].

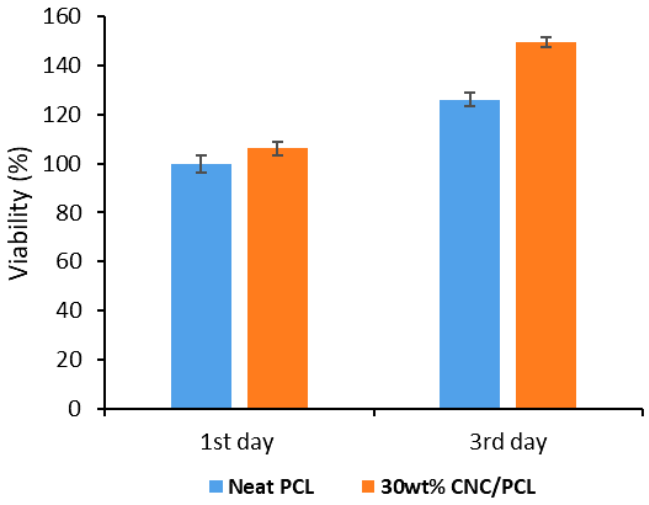

Figure 9 MTT assay cell viability percentage of RAW 246.7 cells in 30 wt% of CNC/PCL and pure PCL electrospun nanofiber scaffolds (Results were expressed as the means ± standard deviation (SD) from triplicates. *P< 0.05 vs control)

4.0 CONCLUSION

In this study, the physical properties such as morphology, hydrophilicity, porosity, thermal stability, and ionic conductivity of CNC/PCL nanofiber scaffold were optimized by changing the concentration of CNC. Results imply that adding CNC into the PCL produced beads-free nanofiber with smaller nanofiber diameter, high hydrophilicity, porosity and improved conductivity, which are optimum for tissue engineering applications. An increase in the weight percentage of CNC in the CNC/PCL composite matrices decreased the fiber diameter and increased the porosity, wettability, and swelling ratio. Notably, 30wt% of CNC added CNC/PCL nanofiber results in optimum wettability around 98.75.6±1.05°, preferable for drug delivery and cell adhesion. On the other hand, when the CNC concentration exceeds 30 wt%, electrospun matrices exhibit high hydrophilicity and fully absorb the water, which may cause higher hydrolytic degradation of the membrane and poor ECM cell binding protein adhesion. In addition, 30 wt% of CNC/PCL nanofiber exhibits the highest conductivity, about 8.13×10^{-6} S/cm, and when the concentration exceeds 30 wt% of CNC, there is a slight reduction in the conductivity. Experimental analysis suggests that the 30 wt% CNC/PCL nanofiber composite scaffold, with moderated hydrophobicity, a higher porosity, and surface conductivity, offers improved cell viability and proliferation. This scaffold demonstrates higher cell viability and proliferation in long-term culture than neat PCL. Therefore, 30 wt% of CNC/PCL nanofiber exhibits optimum physical properties for tissue engineering scaffold applications.

Acknowledgement

The authors acknowledge the financial support from the Ministry of Education Malaysia (MOE) through the Fundamental Research Grant Scheme (600-RMC/FRGS 5/3 (125/2021)) and an internal grant from Universiti Teknologi MARA (600-RMC/KEPU 5/3 (010/2021)). They also extend their gratitude to Progene Link Sdn Bhd, Malaysia, for providing the electrospinning instrument and technical support.

Conflicts of Interest

The author(s) declare(s) that there is no conflict of interest regarding the publication of this paper.

References

[1] Lemos, R. *et al.* 2022. Engineering of Extracellular Matrix-Like Biomaterials at Nano- and Macroscale toward Fabrication of Hierarchical Scaffolds for Bone Tissue Engineering. *Advanced NanoBiomed Research*. Doi: 10.1002/anbr.202100116.

[2] Nikolova, M. P. and Chavali, M. S. 2019. Recent Advances in Biomaterials for 3D Scaffolds: A Review. *Bioactive Materials*. Doi: 10.1016/j.bioactmat.2019.10.005.

[3] Puertas-Bartolomé, M. *et al.* 2021. Emerging Biofabrication Techniques: A Review on Natural Polymers for Biomedical Applications. *Polymers*. Doi: 10.3390/polym13081209.

[4] Hussain, M. H. *et al.* 2023. Surface Modification of Regenerative Cellulose (RC) for Biomedical Applications. In *Regenerated Cellulose and Composites* (eds.Shabbir, M.). Springer Singapore. 79–104.

[5] Peranidze, K. *et al*. 2023. Electrospun Nanomaterials Based on Cellulose and Its Derivatives for Cell Cultures: Recent Developments and Challenges. *Polymers*. Doi: 10.3390/polym15051174.

[6] Agarwal, C. and Csóka, L. 2019. *Surface-modified Cellulose in Biomedical Engineering*. In Materials for Biomedical Engineering (Chapter 6, pp. 215-261). Elsevier. https://doi.org/10.1016/B978-0-12-818431-8.00007-6.

[7] Tortorella, S. *et al*. 2020. Surface-Modified Nanocellulose for Application in Biomedical Engineering and Nanomedicine: A Review. *International Journal of Nanomedicine*. Doi:

10.2147/IJN.S266103.
[8] Courtenay, J. C. *et al.* 2017. Surface Modified Cellulose Scaffolds for Tissue Engineering. *Cellulose*. Doi: 10.1007/s10570-016-1111-y.
[9] Gumrah Dumanli, A. 2017. Nanocellulose and its Composites for Biomedical Applications. *Current Medicinal Chemistry*. Doi: 10.2174/0929867323666161014124008.
[10] Ong, X.-R. *et al.* 2023. Nanocellulose: Recent Advances Toward Biomedical Applications. *Small Science*. Doi: 10.1002/smsc.202200076.
[11] Langari, M. M. *et al.* 2023. Nanocellulose-based Sensors in Medical/clinical Applications: The State-of-the-art Review. *Carbohydrate Polymers*. Doi: 10.1016/j.carbpol.2022.120509.
[12] Bordoni, M. *et al.* 2020. 3D Printed Conductive Nanocellulose Scaffolds for the Differentiation of Human Neuroblastoma Cells. *Cells*. Doi: 10.3390/cells9030682.
[13] Yang, J. *et al.* 2018. Bacterial Cellulose as a Supersoft Neural Interfacing Substrate. *ACS Applied Materials & Interfaces*. Doi: 10.1021/acsami.8b12083.
[14] George, J. and S N, S. 2015. Cellulose Nanocrystals: Synthesis, Functional Properties, and Applications. *Nanotechnology, Science and Applications*. Doi: 10.2147/NSA.S64386.
[15] Abu Bakar, N. F. *et al.* 2022. Nanocellulose from Oil Palm Mesocarp Fiber using Hydrothermal Treatment with Low Concentration of Oxalic Acid. *Materials Today: Proceedings*. Doi: 10.1016/j.matpr.2021.09.357.
[16] Salimi, S. *et al.* 2019. Production of Nanocellulose and Its Applications in Drug Delivery: A Critical Review. *ACS Sustainable Chemistry & Engineering*. Doi: 10.1021/acssuschemeng.9b02744.
[17] Lugoloobi, I. *et al.* 2021. Cellulose Nanocrystals in Cancer Diagnostics and Treatment. *Journal of Controlled Release*. Doi: 10.1016/j.jconrel.2021.06.004.
[18] Szustak, M. and Gendaszewska-Darmach, E. 2021. Nanocellulose-Based Scaffolds for Chondrogenic Differentiation and Expansion. *Frontiers in Bioengineering and Biotechnology*. Doi: 10.3389/fbioe.2021.736213.
[19] Janmohammadi, M. *et al.* 2023. Cellulose-based Composite Scaffolds for Bone Tissue Engineering and Localized Drug Delivery. *Bioactive Materials*. Doi: 10.1016/j.bioactmat.2022.05.018.
[20] Hussain, M. H. *et al.* 2023. Electrospun Polyetherimide Nanofibers with Reduced Graphene Oxide-zeolitic Imidazolate Framework for Conductivity Improvement. *Emergent Materials*. Doi: 10.1007/s42247-022-00410-x.
[21] Su, Y. *et al.* 2021. 3D Electrospun Synthetic Extracellular Matrix for Tissue Regeneration. *Small Science*. Doi: 10.1002/smsc.202100003.
[22] Sheng, L. *et al.* 2014. Electrospun Cellulose Nanocrystals/Polycaprolactone Nanocomposite Fiber Mats. *Journal of Macromolecular Science, Part B*. Doi: 10.1080/00222348.2013.861311.
[23] Hivechi, A. *et al.* 2019. Drug Release and Biodegradability of Electrospun Cellulose Nanocrystal Reinforced Polycaprolactone. *Materials Science and Engineering: C*. Doi: 10.1016/j.msec.2018.10.037.
[24] Bellani, C. F. *et al*. 2016. Morphological, Thermal, and Mechanical Properties of Poly(ε-caprolactone)/poly(ε-caprolactone)-grafted-cellulose Nanocrystals Mats Produced by Electrospinning. *Journal of Applied Polymer Science*. Doi: 10.1002/app.43445.
[25] Zoppe, J. O. *et al.* 2009. Reinforcing Poly(ε-caprolactone) Nanofibers with Cellulose Nanocrystals. *ACS Applied Materials & Interfaces*. Doi: 10.1021/am9003705.
[26] Hivechi, A. *et al.* 2021. Cellulose Nanocrystal Effect on Crystallization Kinetics and Biological Properties of Electrospun Polycaprolactone. *Materials Science and Engineering: C*. Doi: 10.1016/j.msec.2020.111855.
[27] Huang, R. *et al.* 2020. Bio-Composites Consisting of Cellulose Nanofibers and Na+ Montmorillonite Clay: Morphology and Performance Property. *Polymers*. Doi: 10.3390/polym12071448.
[28] Ye, P. *et al*. 2020. Long-Term Effect against Methicillin-Resistant Staphylococcus aureus of Emodin Released from Coaxial Electrospinning Nanofiber Membranes with a Biphasic Profile. *Biomolecules*. Doi: 10.3390/biom10030362.
[29] Ko, S. W. *et al.* 201). Analysis of Drug Release Behavior Utilizing the Swelling Characteristics of Cellulosic Nanofibers. *Polymers*. Doi: 10.3390/polym11091376.
[30] Abu Bakar, N. F. *et al.* 2021. Electrospun Polyetherimide-Graphene Oxide Nanofiber Electrodes for Enhanced Conductivity. *Journal of Fiber Science and Technology*. Doi: 10.2115/fiberst.2021-0013.
[31] Sousa, I. *et al.* 2013. PCL Scaffolds with Collagen Bioactivator for Applications in Tissue Engineering. *Procedia Engineering*. Doi: 10.1016/j.proeng.2013.05.122.
[32] Safi, I. N. *et al.* 2020. Preparing Polycaprolactone Scaffolds using Electrospinning Technique for Construction of Artificial Periodontal Ligament Tissue. *Journal of Taibah University Medical Sciences*. Doi: 10.1016/j.jtumed.2020.07.007.
[33] Anjum, S. *et al.* 2023. Multifunctional Electrospun Nanofibrous Scaffold Enriched with Alendronate and Hydroxyapatite for Balancing Osteogenic and Osteoclast Activity to Promote Bone Regeneration. *Frontiers in Bioengineering and Biotechnology*. Doi: 10.3389/fbioe.2023.1302594.
[34] Liang, H. *et al.* 2020. 3D-printed porous Titanium Scaffolds Incorporating Niobium for High Bone Regeneration Capacity. *Materials & Design*. Doi: 10.1016/j.matdes.2020.108890.
[35] Angammana, C. J. and Jayaram, S. H. 2011. Analysis of the Effects of Solution Conductivity on Electrospinning Process and Fiber Morphology. *IEEE Transactions on Industry Applications*. Doi: 10.1109/TIA.2011.2127431.
[36] Kyriakides, T. R. 2015. Molecular Events at Tissue–Biomaterial Interface. In *Host Response to Biomaterials*. Elsevier. 81–116.
[37] Okano, T. *et al.* 1995. Mechanism of Cell Detachment from Temperature-modulated, Hydrophilic–hydrophobic Polymer Surfaces. *The Biomaterials: Silver Jubilee Compendium*. 16: 109–115.
[38] Magiera, A. *et al.* 2018. Degradation Behavior of Electrospun PLA and PLA/CNT Nanofibres in Aqueous Environment. *Journal of Nanomaterials*. Doi: 10.1155/2018/8796583.
[39] Ghasemiyeh, P. and Mohammadi-Samani, S. 2021. Polymers Blending as Release Modulating Tool in Drug Delivery. *Frontiers in Materials*. Doi: 10.3389/fmats.2021.752813.
[40] Sarmadi, M. *et al.* 2017. Utilization of Molecular Dynamics Simulation Coupled with Experimental Assays to Optimize Biocompatibility of an Electrospun PCL/PVA Scaffold. *PLOS ONE*. Doi: 10.1371/journal.pone.0169451.
[41] Mitra, S. P. 2020. Protein Adsorption on Biomaterial Surfaces: Subsequent Conformational and Biological Consequences – A Review. *Journal of Surface Science and Technology*. Doi: 10.18311/jsst/2020/23282.
[42] Kramschuster, A. and Turng, L.-S. 2013. Fabrication of Tissue Engineering Scaffolds. *Handbook of Biopolymers and Biodegradable Plastics*. Elsevier. 427–446.
[43] Turnbull, G. *et al.* 2018. 3D Bioactive Composite Scaffolds for Bone Tissue Engineering. *Bioactive Materials*. Doi: 10.1016/j.bioactmat.2017.10.001.
[44] Pan, J. *et al.* 2014. Preparation and Characterization of Electrospun PLCL/Poloxamer Nanofibers and Dextran/Gelatin Hydrogels for Skin Tissue Engineering. *PLoS ONE*. Doi: 10.1371/journal.pone.0112885.
[45] Gibril, M. E. *et al.* 2022. Effect of Nanocrystalline Cellulose and Zinc Oxide Hybrid Organic–inorganic Nanofiller on the Physical Properties of Polycaprolactone Nanocomposite Films. *Microsystem Technologies*. Doi: 10.1007/s00542-019-04497-x.
[46] Sikorski, P. 2020. Electroconductive Scaffolds for Tissue Engineering Applications. *Biomaterials Science*. Doi: 10.1039/D0BM01176B.
[47] Marsudi, M. A. *et al.* 2021. Conductive Polymeric-Based

Electroactive Scaffolds for Tissue Engineering Applications: Current Progress and Challenges from Biomaterials and Manufacturing Perspectives. *International Journal of Molecular Sciences*. Doi: 10.3390/ijms222111543.
[48] Yang, H. *Ion Transport in Cross-linked Nanocellulose Membranes*. Linköping University.
[49] Huang, X. *et al.* 2023. A Facile One-Pot Preparation and Properties of Nanocellulose-Reinforced Ionic Conductive Hydrogels. *Molecules*. Doi: 10.3390/molecules28031301.
[50] Scalera, F. *et al.* 2021. Sustainable Chitosan-based Electrical Responsive Scaffolds for Tissue Engineering Applications. *Sustainable Materials and Technologies*. Doi: 10.1016/j.susmat.2021.e00260.
[51] Serafin, A. *et al.* 2022. Electroconductive PEDOT Nanoparticle Integrated Scaffolds for Spinal Cord Tissue repair. *Biomaterials Research*. Doi: 10.1186/s40824-022-00310-5.
[52] Flamourakis, G. *et al.* 2023. High-resolution Lightweight and Multifunctional 3D Printed Scaffolds for Cell Studies. *Results in Materials*. Doi: 10.1016/j.rinma.2023.100393.
[53] Zhang, Y. *et al*. 2022. A Tailored Bioactive 3D Porous Poly(lactic-acid)-exosome Scaffold with Osteo-immunomodulatory and Osteogenic Differentiation Properties. *Journal of Biological Engineering*. Doi: 10.1186/s13036-022-00301-z.
[54] Dutta, S. D. *et al.* 2019. In Vitro Biocompatibility of Electrospun Poly(ε -Caprolactone)/Cellulose Nanocrystals-Nanofibers for Tissue Engineering. *Journal of Nanomaterials*. Doi: 10.1155/2019/2061545.